

A cationic Zn^{II} porphyrazine induces a stable parallel G-quadruplex conformation in human telomeric DNA

Ilse Manet,^{a*} Francesco Manoli,^a Maria Pia Donzello,^{b*} Elisa Viola,^b Giuseppina Andreano^c, Annalisa Masi^c, Luciano Cellai,^c and Sandra Monti^{a*}

^a *ISOF, Consiglio Nazionale delle Ricerche, via Gobetti 101, 40129 Bologna, Italy.*

^b *Dipartimento di Chimica, Università degli Studi di Roma "La Sapienza", P.le A. Moro 5, 00185 Roma, Italy*

^c *IC, Consiglio Nazionale delle Ricerche, Area della Ricerca di Roma 1, 00015 Monterotondo Scalo, Rome, Italy.*

Supplementary information

S1) Sample preparation

The buffer used for the spectroscopic measurements contained 10 mM TRIS, 1 mM EDTA and 100 mM KCl. Excess of K^+ was used in order to mimic physiological conditions of cellular environments where K^+ is abundant. pH was corrected to a value of 7.4 with aliquots of HCl 3N. Only for the melting experiments a 10 mM sodium cacodylate buffer with 100 mM KCl was used. The pH of the buffer was corrected to a value of 7.38 with HCl 0.1 N. The telomeric sequence 5'-d[AGGG(TTAGGG)₃]-3' (22-mer) was prepared by automated synthesis according to standard procedures. The 22-mer stock solution was heated at 90°C for 15 min and then cooled down to room temperature before use. The iodide salt of tetrakis-2,3-[5,6-di(2-(*N*-methyl)pyridiniumyl)pyrazino]-porphyrinato-Zn^{II}, called [PzZn]⁸⁺, was dissolved up to a concentration of 2×10^{-5} M in these buffers. Aliquots of [PzZn]⁸⁺ and 22-mer solutions in the same buffer were mixed together to prepare solutions of varying molar ratio. Water was purified by passage through a Millipore MilliQ system (Millipore SpA, Milan, Italy). All the solvents were spectroscopy grade.

S2) Spectroscopic measurements

UV-vis absorption spectra were recorded on a Perkin-Elmer λ 9 spectrophotometer. Fluorescence spectra were obtained on a Spex Fluorolog 111A spectrofluorimeter. Right angle detection was used. CD spectra were obtained with a Jasco J-715 spectropolarimeter. Each spectrum was registered accumulating three scans with scan rate of 100 nm/min for the visible and 50 nm/min for the UV and integration time of 1 s to improve the signal-to-noise ratio. In the 500-750 nm range 6 accumulations were performed with a integration time of 2s and scan rate of 50 nm/min. All the measurements were carried out at 295 K. All experiments were carried out in quartz cuvetts of 1.0, 0.5, 0.2 cm path length. For the melting experiment temperature was changed in 1°C steps and the measurement was performed every 5 minutes. Ellipticity values at 268 and 290 nm were the mean of three readings using a band width of 2 nm and a response time of 8 seconds. Error is estimated in ± 0.05 mdeg.

S3) Fluorescence of $[\text{PzZn}]^{8+}$

Fig. S1 shows the fluorescence spectrum of 3×10^{-6} M solution of $[\text{PzZn}]^{8+}$ alone and with equimolar concentration of 22-mer in 0.01 M TRIS buffer of pH 7.4 with 0.1 M KCl. Excitation has been performed at 645 nm. The fluorescence spectrum resembles that reported in literature for other porphyrazines.¹ Feasibility of photoinduced intermolecular electron transfer as quenching mechanism can be evaluated calculating the Gibbs free energy for the formation of the solvent-separated radical ion pair with the Rehm-Weller equation.² Considering $E(\text{dGMP}^{\cdot-}/\text{dGMP}) = 1.29$ V,³ and $E(\text{PzZn}^{8+}/\text{PzZn}^{7+}) \cong 0.144$ V⁴ vs. NHE, and ${}^1\text{PzZn}^{8+*} = 1.94$ eV (onset at 640 nm) and neglecting coulombic terms, $\Delta G(\text{electron transfer})$ is calculated to be ~ -0.79 eV so that the process results thermodynamically allowed in the excited singlet state.

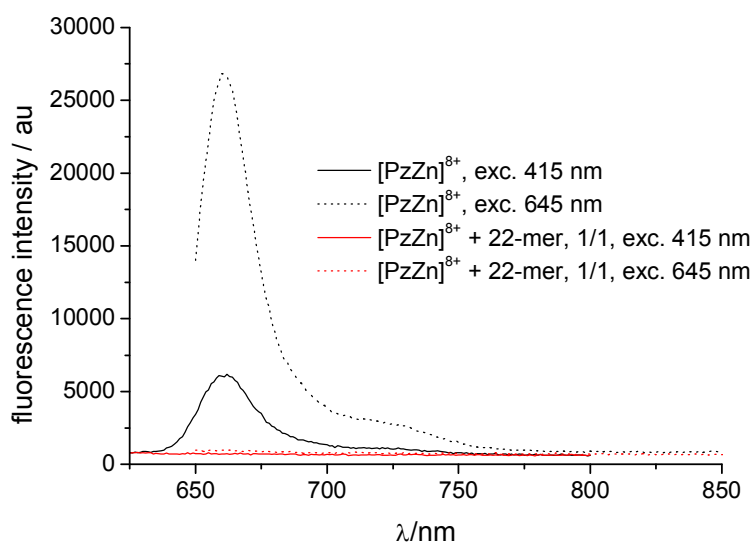


Fig. S1. Fluorescence spectra of $[\text{PzZn}]^{8+}$ with and without 22-mer exciting the solution at 645 and 415 nm.

S4) Titration of the 22-mer with $[\text{PzZn}]^{8+}$ monitoring CD at 295 K in the 220-350 nm range

In the article we report the figures of the ellipticity changes observed increasing the ligand concentration for the freshly prepared solutions and for the solutions kept in the dark three days at room temperature and then heated for 10 minutes at 85°C. The graph below (Fig. S2) shows the ellipticity changes of these solutions after conservation in the dark.

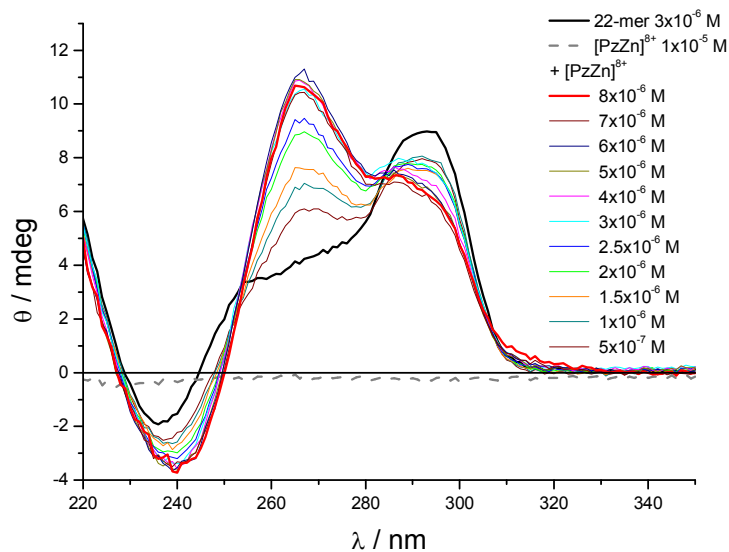


Fig. S2 Ellipticity (θ) of 3.0×10^{-6} M 22-mer solutions containing increasing concentrations of $[\text{PzZn}]^{8+}$ in 10 mM TRIS buffer with 0.1 M KCl, pH 7.4, $d=1.0$ cm, 295 K; $[\text{PzZn}]^{8+} = (0.5, 1, 1.5, 2, 2.5, 3, 4, 5, 6, 7, 8) \times 10^{-6}$ M; mixtures kept in the dark for three days at room temperature.

S5) Melting of 22-mer

Fig. S3 shows the melting spectra of a 2.0×10^{-6} M solution of 22-mer in 0.01 M cacodylate buffer with 0.1 M KCl.

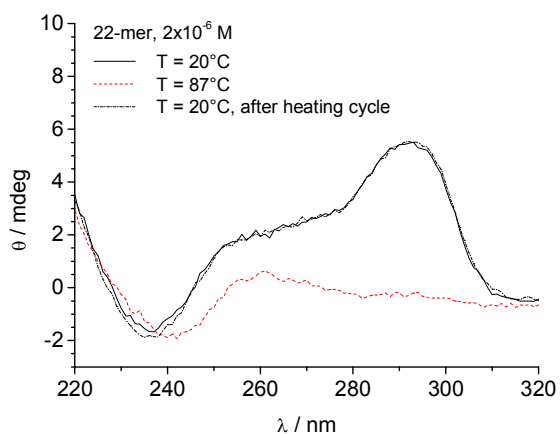


Fig. S3.

S6). Global analysis of equilibrium spectroscopic data with Singular Value Decomposition and non linear regression modelling.

This application was performed using the commercial SPECFIT/32TM program, based on the publications of A. Zuberbühler at the University of Basel, Switzerland.^{5, 6} Multiwavelength spectroscopic data sets are arranged in matrix form \mathbf{Y} , where a number N_w of wavelengths and a

number N_m of corresponding measured spectroscopic signals are in columns, whereas ligand and receptor concentrations are in rows. Thus each element of the data matrix Y_{ij} corresponds to a wavelength j and an experimental quantity (absorbance, circular dichroism, fluorescence intensity) for a given couple of concentrations i of ligand and receptor (typically in our experiments one of them is kept constant). A least square best estimator Y' of the original data Y is reconstructed as the eigenvector representation $Y' = U \times S \times V$, where S is a vector that contains the relative weights of the significant eigenvectors (N_e , number of significant eigenvectors), U is a matrix ($N_m \times N_e$) of concentration eigenvectors ($U^T \times U = 1$, orthonormal) and V ($N_e \times N_w$) is a matrix of spectroscopic eigenvectors ($V \times V^T$, orthonormal). This Y' matrix contains less noise than Y because the SVD decomposition procedure can factor random noise from the principal components. This reconstructed data matrix Y' is utilized in the global fitting instead of the original data matrix Y . Complexation equilibria are solved assuming a complexation model (i.e. contemporary presence of complexes of given stoichiometries in equilibrium with free species in solution) and optimizing the numeric combination of all the spectroscopic contributions to best reproduce the Y' signals. Optimization is performed by the least square method, using the Levenberg-Marquardt algorithm, for all the explored wavelengths and ligand-receptor concentration couples. The optimized parameters are the association constants. The spectra of the equilibrium components are also extracted.

We applied this method to the analysis of the circular dichroism data for titration of $[PzZn]^{8+}$ with 22-mer, represented in Fig. 4 of the manuscript. The SVD analysis of the data of the UV CD titration resulted to be the following:

[FACTOR ANALYSIS]

Tolerance = 1.000E-09

Max.Factors = 10

Num.Factors = 5

Significant = 4

Eigen Noise = 1.380E-01

Exp't Noise = 2.761E-02

#	Eigenvalue	Square Sum	Residual	Prediction
1	6.631E+05	1.491E+04	3.158E+00	Data Vector
2	1.454E+04	3.694E+02	4.973E-01	Data Vector

3	2.338E+02	1.357E+02	3.015E-01	Data Vector
4	1.072E+02	2.843E+01	1.380E-01	Data Vector
5	1.705E+01	1.138E+01	8.735E-02	Probably Noise

The SVD analysis of the data of the visible CD titration resulted to be the following:

[FACTOR ANALYSIS]

Tolerance = 1.000E-09

Max.Factors = 10

Num.Factors = 5

Significant = 1

Eigen Noise = 1.006E-01

Exp't Noise = 2.012E-01

#	Eigenvalue	Square Sum	Residual	Prediction
1	1.967E+03	4.765E+01	1.006E-01	Data Vector
2	2.441E+01	2.324E+01	7.027E-02	Possibly Data
3	4.842E+00	1.840E+01	6.253E-02	Probably Noise
4	4.194E+00	1.421E+01	5.495E-02	Probably Noise
5	3.035E+00	1.117E+01	4.873E-02	Probably Noise

Several binding models were tested. The fits were evaluated on the basis of their Durbin-Watson (DW) factors and the relative error. The DW test is very useful to check for the presence of auto-correlation in the residuals. This method is recommended for systematic misfit errors that can arise in titration experiments. It examines the tendency of successive residual errors to be correlated. The Durbin-Watson statistics ranges from 0.0 to 4.0, with an optimal mid-point value of 2.0 for uncorrelated residuals (i.e., no systematic misfit). In contrast to the χ^2 (Chi-squared) statistics, which requires the noise in the experimental data is random and normally distributed, the DW factor is meaningful even when the noise level in the data set is low. Since the factorized data usually have a significantly lower noise level than the original data, DW test is ideal for the present type of data.

From SPECFIT analysis of both the UV and Vis CD titration data of Fig. 4 in the manuscript the best complexation model on the basis of the DW factors resulted to be that with 1:1 and 2:1 $[\text{PzZn}]^{8+}$:22-mer complexes, assuming $[\text{PzZn}]^{8+}$ is involved in a dimerization equilibrium with constant $\log(K_d/\text{M}^{-1}) = 6.6 \pm 0.5$ (see paragraph S7 below). This constant was kept fixed in the calculation. The best fit parameters were $\log(K_{11}/\text{M}^{-1}) = 6.4 \pm 0.3$ and $\log(K_{21}/\text{M}^{-2}) = 12.4 \pm 0.4$ (Durbin Watson factor = 1.9) from the CD UV titration data and $\log(K_{11}/\text{M}^{-1}) = 6.2 \pm 0.2$ and $\log(K_{21}/\text{M}^{-2}) = 13.1 \pm 0.4$ (Durbin Watson factor = 1.5) from the CD Vis titration data in the 320-600

nm range. For the 600-750 nm range we obtained $\log(K_{11}/M^{-1}) = 6.2$ (fixed) and $\log(K_{21}/M^{-2}) = 13.1 \pm 0.4$ (Durbin Watson factor = 2.4). An example of the quality of the agreement between the experimental data and the best fits is shown in Figures S4 and S5. Global analysis of the combined sets of data for the whole UV-Vis spectral range confirmed the reliability of the binding model affording similar association constants ($\log(K_{11}/M^{-1}) = 6.4 \pm 0.4$ and $\log(K_{21}/M^{-2}) = 12.4 \pm 0.4$ (Durbin Watson factor = 2.4).

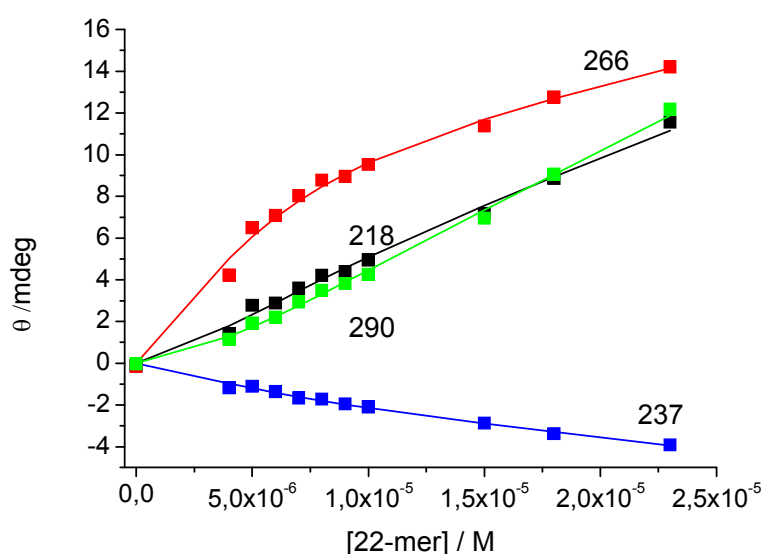


Fig. S4. Ellipticity (θ) at key wavelengths (nm) of a 8×10^{-6} M $[\text{PzZn}]^{8+}$ solutions with increasing 22mer concentration $(0.5\text{-}2.3) \times 10^{-5}$ M in TRIS/KCl buffer of pH 7.4 at 295 K, $d = 0.2$ cm; Symbols are experimental values; lines represent best fit values for $\log(K_{11}/M^{-1}) = 6.4 \pm 0.3$ and $\log(K_{21}/M^{-2}) = 12.4 \pm 0.4$.

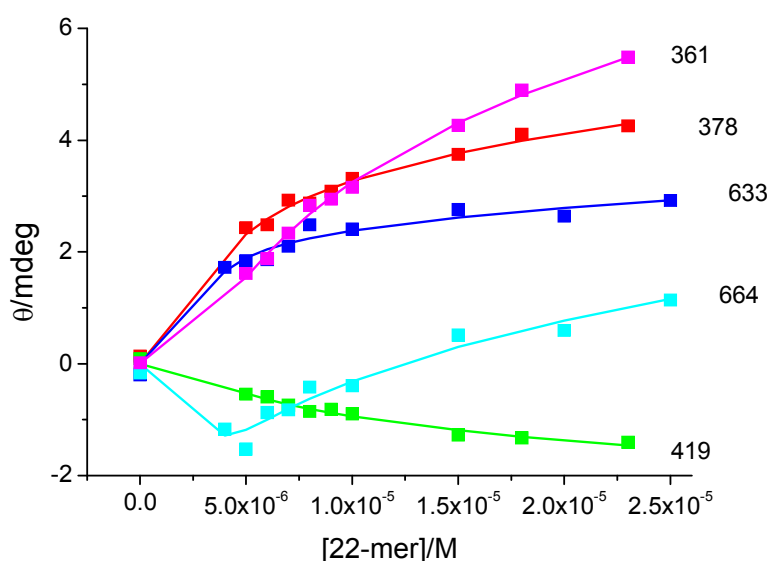


Fig. S5. Ellipticity (θ) at key wavelengths (nm) of a 0.8×10^{-5} M $[\text{PzZn}]^{8+}$ solution with increasing 22mer concentration $(0.5\text{-}2.3) \times 10^{-5}$ M in TRIS/KCl buffer of pH 7.4 at 295 K, $d = 2$ cm; Symbols are experimental values; lines represent best fit values for $\log(K_{11}/M^{-1}) = 6.2 \pm 0.2$ and $\log(K_{21}/M^{-2}) = 13.1 \pm 0.4$.

We report in Fig. S6 the evolution of the concentrations of the various species in solution assuming $\log(K_{11}/M^{-1}) = 6.4$ and $\log(K_{21}/M^{-2}) = 12.4$.

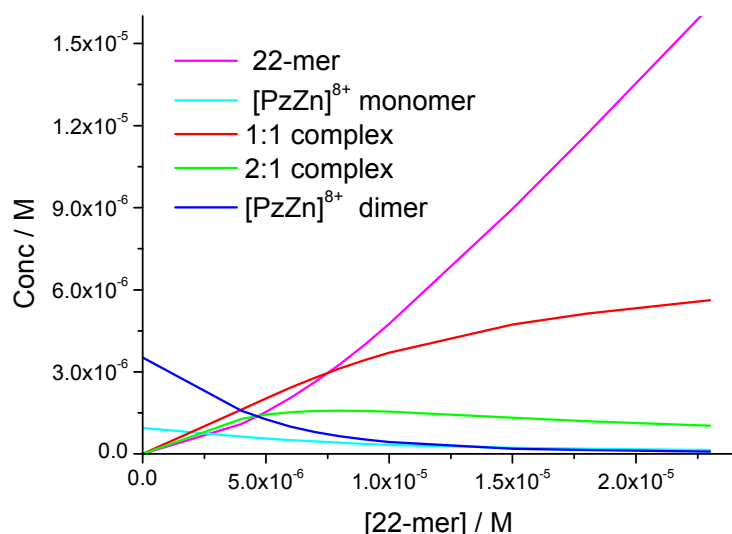


Fig. S6. Evolution of the concentrations of the various species in solution for titration of a 0.8×10^{-5} M $[\text{PzZn}]^{8+}$ solution with 22mer in TRIS/KCl buffer of pH 7.4 at 295 K, assuming $\log(K_{11}/M^{-1}) = 6.4$ and $\log(K_{21}/M^{-2}) = 12.4$.

S7) Dimerization equilibrium of $[\text{PzZn}]^{8+}$

It was previously shown that $[\text{PzZn}]^{8+}$ tends to aggregate in water solution.⁴ In the absorption spectrum of $[\text{PzZn}]^{8+}$ in water the Q band has a maximum at 625 nm with a shoulder at 650 nm and these features have been attributed to the presence of a dimeric species. In DMF/HCl ($[\text{HCl}] = 1 \times 10^{-4}$ M) $[\text{PzZn}]^{8+}$ is present as monomeric species with absorption maximum of the Q band at 665 nm. (Fig. S7).

We performed a dilution experiment in aqueous medium in the range 9×10^{-7} M \div 1.65×10^{-5} M (Fig. S8). Analysis using Specfit/32 yielded an apparent dimerization constant $\log(K_d/M^{-1}) = 6.6 \pm 0.5$ (Durbin-Watson factor of 1.3, relative error of fit 1.2%). The calculated spectra of the monomeric and dimeric species in fig. S9 show the change in the relative intensity of the peaks at 625 and 650 from dimer to monomer. In spite of the different spectral profiles in H_2O and DMF, the integrated areas of the Q band of the monomeric species are similar in these two solvents.

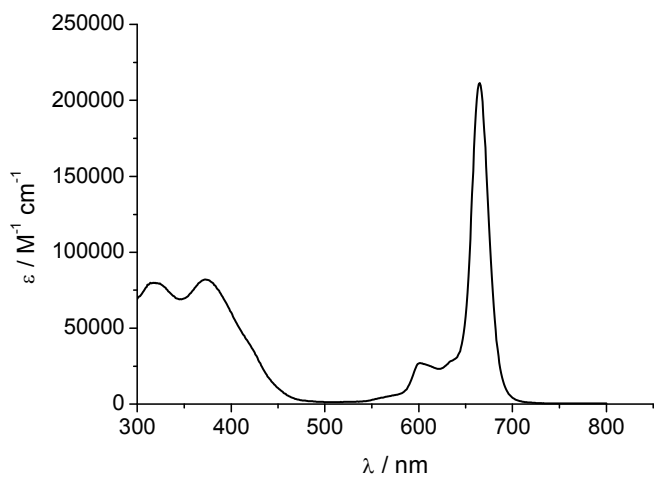


Fig. S7. Absorption spectrum of $[\text{PzZn}]^{8+}$ in DMF/HCl ($[\text{HCl}] = 1 \times 10^{-4} \text{ M}$).

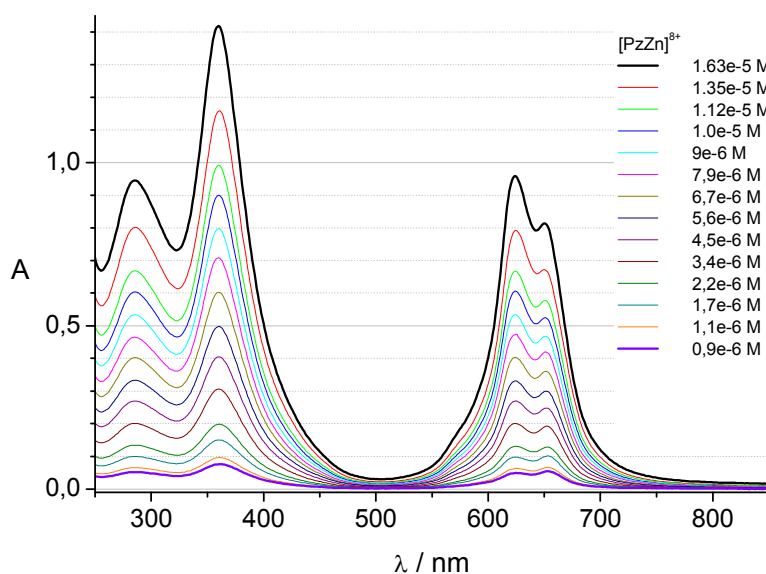


Fig. S8. Absorbance changes upon dilution of $2 \times 10^{-5} \text{ M}$ $[\text{PzZn}]^{8+}$ solution in 0.01 M TRIS with 0.1 M KCl at pH 7.4.

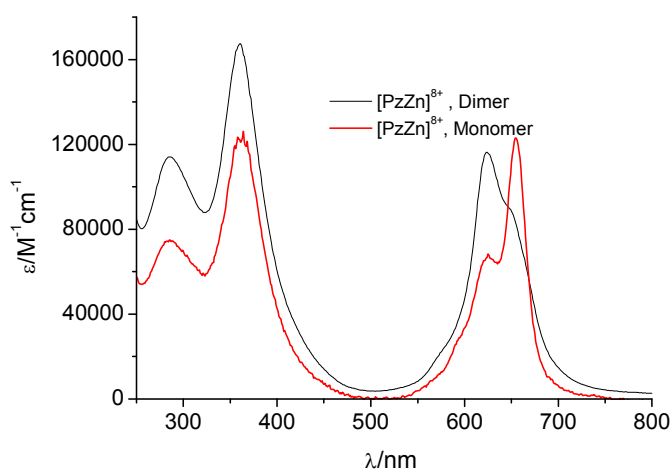


Fig. S9. Calculated absorption spectrum [PzZn]⁸⁺ in monomeric and dimeric form.

Bibliography

1. T. C. Tempesti, J. C. Stockert and E. N. Durantini, *J. Phys. Chem. B*, 2008, **112**, 15701-15707.
2. D. Rehm and A. Weller, *Israel Journal of Chemistry*, 1970, **8**, 13.
3. S. Steenken and S. V. Jovanovic, *J. Am. Chem. Soc.*, 1997, **119**, 617-618.
4. C. Bergami, M. P. Donzello, F. Monacelli, C. Ercolani and K. M. Kadish, *Inorganic Chemistry*, 2005, **44**, 9862-9873.
5. H. Gampp, M. Maeder, C. J. Meyer and A. D. Zuberbuhler, *Talanta*, 1985, **32**, 95-101.
6. H. Gampp, M. Maeder, C. J. Meyer and A. D. Zuberbuhler, *Talanta*, 1985, **32**, 257-264.